

# UCSF

## UC San Francisco Previously Published Works

### Title

Developmental sensory experience balances cortical excitation and inhibition.

### Permalink

<https://escholarship.org/uc/item/2578s610>

### Journal

Nature, 465(7300)

### ISSN

0028-0836

### Authors

Dornn, Anja L  
Yuan, Kexin  
Barker, Alison J  
[et al.](#)

### Publication Date

2010-06-01

### DOI

10.1038/nature09119

Peer reviewed



Published in final edited form as:

Nature. 2010 June 17; 465(7300): 932–936. doi:10.1038/nature09119.

## Developmental sensory experience balances cortical excitation and inhibition

Anja L. Dornn<sup>1,\*</sup>, Kexin Yuan<sup>2,\*</sup>, Alison J. Barker<sup>2</sup>, Christoph E. Schreiner<sup>2</sup>, and Robert C. Froemke<sup>3</sup>

<sup>1</sup>Department of Neuroscience, Max-Delbrück Center for Molecular Medicine, NeuroCure, NWFZ, Berlin, Germany

<sup>2</sup>Coleman Memorial Laboratory and W.M. Keck Foundation Center for Integrative Neuroscience, Department of Otolaryngology, University of California, San Francisco, California, USA

<sup>3</sup>Molecular Neurobiology Program, The Helen and Martin Kimmel Center for Biology and Medicine at the Skirball Institute of Biomolecular Medicine, Departments of Otolaryngology, Physiology and Neuroscience, New York University School of Medicine, New York, New York, USA.

### Abstract

Early in life, neural circuits are highly susceptible to outside influences. The organization of primary auditory cortex (AI) in particular is governed by acoustic experience during the critical period, an epoch near the beginning of postnatal development throughout which cortical synapses and networks are especially plastic<sup>1-8</sup>. This neonatal sensitivity to the pattern of sensory inputs is believed to be essential for constructing stable and adequately adapted representations of the auditory world and for the acquisition of language skills by children<sup>5,9,10</sup>. One important principle of synaptic organization in mature brains is the balance between excitation and inhibition, which controls receptive field structure and spatiotemporal flow of neural activity<sup>11-15</sup>, but it is unknown how and when this excitatory-inhibitory balance is initially established and calibrated. Here we used whole-cell recording to determine the processes underlying the development of synaptic receptive fields in rat AI. We found that, immediately after hearing onset, sensory-evoked excitatory and inhibitory responses were equally strong, although inhibition was less stimulus-selective and mismatched with excitation. However, during the third week of postnatal development, excitation and inhibition became highly correlated. Patterned sensory stimulation drove coordinated synaptic changes across receptive fields, rapidly improved excitatory-inhibitory coupling, and prevented further exposure-induced modifications.

Users may view, print, copy, download and text and data- mine the content in such documents, for the purposes of academic research, subject always to the full Conditions of use: [http://www.nature.com/authors/editorial\\_policies/license.html#terms](http://www.nature.com/authors/editorial_policies/license.html#terms)

Correspondence should be addressed to: Robert C. Froemke Phone: 212-263-7595, [robert.froemke@med.nyu.edu](mailto:robert.froemke@med.nyu.edu).

\*These authors contributed equally to this work.

**Author contributions** A.L.D., K.Y., A.J.B., and R.C.F. performed the experiments and analyses. All authors discussed the experiments and contributed to the manuscript.

**Supplementary Information** is linked to the online version of the paper at [www.nature.com/nature](http://www.nature.com/nature).

**Author information** Reprints and permissions information is available at [npg.nature.com/reprintsandpermissions](http://npg.nature.com/reprintsandpermissions).

The authors declare that they have no competing financial interests.

Thus the pace of cortical synaptic receptive field development is set by progressive, experience-dependent refinement of intracortical inhibition.

---

Synaptic development in rodent AI generally occurs over the first postnatal month<sup>16,17</sup>. During this time, the nascent organization of AI can be extensively altered by passive exposure to structured auditory stimuli, such as repetitive sequences of pure tones at a given frequency<sup>3,7</sup>. Recent studies indicate that inhibitory circuits play key roles in this process, first enabling and eventually limiting the extent of receptive field plasticity<sup>6,18,19</sup>. However, it is unclear how inhibition at the cellular and network levels is developmentally coordinated to shape receptive field selectivity and control cortical plasticity. As sensory-evoked subthreshold responses cannot yet be directly measured optically, by extracellular recording *in vivo*, or by intracellular recording *in vitro*, here we used *in vivo* whole-cell recording to study synaptic organization and plasticity of developing AI.

We made 107 whole-cell voltage-clamp recordings from rat AI neurons *in vivo*. Recordings were obtained from postnatal day 12 (P12) to P30 and from adult animals. Frequency tuning profiles of AI neurons were measured with pure tones at different holding potentials to compute excitatory and inhibitory conductances<sup>11-15</sup>.

We found that, in young animals, excitatory and inhibitory frequency tuning profiles were individually present but uncoupled, unlike the highly correlated and balanced excitation and inhibition measured in neurons from older animals. For example, at P14 (Fig. 1a, Supplementary Fig 1), although substantial tone-evoked excitatory and inhibitory responses were observed (Fig. 1a, top), magnitudes of excitation and inhibition were uncorrelated across frequencies (Fig. 1a, bottom;  $r: -0.01$ ). This was in contrast to recordings from adults, in which excitatory inputs were balanced by a proportional amount of co-tuned inhibition (Fig. 1b;  $r: 0.87$ ; Supplementary Fig. 2).

By P21, the correlation between excitatory and inhibitory inputs had increased (Fig. 1c). Initially after hearing onset (~P12), excitation and inhibition were generally mismatched. During P15-P21, excitatory and inhibitory responses were partially but not strongly correlated, relative to balanced tuning observed in adult AI. Moreover, stimuli evoking maximal excitation and inhibition in a given cell differed during development. In mature AI, excitatory and inhibitory best frequencies were approximately the same, while in young AI, peak excitatory and inhibitory responses were over an octave apart on average (Fig. 1d).

This early imbalance between synaptic inputs was due to low selectivity of inhibitory tuning. To measure sharpness of tuning, we normalized tuning curves and used linear slopes (Supplementary Fig. 3) and standard deviations of Gaussian fits (Fig. 2) as selectivity indices for excitation and inhibition. For the P14 cell shown in Figure 1a, inhibition was less tuned than excitation (Fig. 2a), in contrast to the sharper inhibitory tuning observed in older animals (Fig. 2b), as previously suggested<sup>19</sup>.

Development of inhibitory frequency tuning was delayed relative to excitation (Fig. 2c,d). Sharpness of excitatory tuning was close to adult levels by ~P15, but inhibitory tuning was slower to emerge, eventually maturing around P25-P30. Thus early in cortical development,

inhibitory inputs are poorly tuned for spectral features of sensory stimuli, leading to imbalanced synaptic tuning profiles and accounting for high-threshold or less-structured spiking receptive fields and frequency maps reported in young animals<sup>7,15,19,20</sup>.

A generally low inhibitory tonus at the onset of AI development might account for nonselective frequency tuning of inhibition. However, while many aspects of neuronal excitability and synaptic transmission change over development<sup>17</sup> (Supplementary Figs. 4,5), average strengths of tone-evoked inhibitory conductances were similar in young and adults, in terms of absolute magnitude (Supplementary Fig. 3d) and relative to excitation (Fig. 2d). This suggests that the pace of the AI critical period is not determined solely at the level of individual synapses, e.g., by gross strengthening of GABAergic inhibition. Instead, changes of inhibitory transmission must be coordinated across the cortical network, to shape the tuning of intracortical inhibition throughout the entire receptive field in such a way as to match and balance the overall structure of excitatory inputs.

What factors contribute to refinement of excitatory-inhibitory balance during the AI critical period? Sensory experience is known to control development of cortical receptive fields and networks<sup>3,4,6,7,18,21</sup>. We therefore examined the effect of patterned sensory stimulation on maturation of synaptic frequency tuning.

We first measured baseline tuning before repetitively playing a tone of a specific frequency for 3-5 minutes (patterned stimulation). After 5-10 minutes, we assessed changes to synaptic tuning. In young but not adult animals, patterned stimulation led to rapid increases in synaptic strength (Fig. 3), enhancing excitatory-inhibitory balance, shortening response latency (Supplementary Fig. 4f), and persisting for 30+ minutes.

Thus the major features of AI synaptic receptive field development are a progressive balancing of excitation and inhibition, driven by sharpening of initially poorly-tuned inhibitory inputs, and susceptibility to exposure-induced synaptic modifications that enhance excitatory-inhibitory coupling. Given their similar age dependence, we hypothesized that there was a relationship between formation of excitatory-inhibitory balance and the age window for synaptic plasticity. We noticed that patterned stimulation led to changes not only at the presented input, but also across other frequencies. Consequently, excitatory and inhibitory tuning profiles became more similar. Although these synaptic responses exhibited complex spectrotemporal evolution, there were three general principles of developmental synaptic receptive field modification induced by patterned stimulation.

First, potentiation of excitation and inhibition was not limited to the presented frequency alone, but spread to frequencies within one octave (Fig. 4a). Second, excitation and inhibition depressed at their respective best frequencies (Fig. 4b). Third, these positive and negative changes to multiple inputs cooperated to increase excitatory-inhibitory balance (Fig. 4c).

Changes at stimuli other than the presented frequency were predominant in enhancing excitatory-inhibitory coupling. Considered separately, changes to the presented frequency did not greatly increase correlation (Fig. 4d, “presented only”), while changes to other inputs could entirely account for increased correlation (Fig. 4d, “unpresented only”).

Acceleration of frequency tuning was specific for pure tones. Stimulation with white noise (Supplementary Fig. 6) did not affect excitatory-inhibitory balance, regardless of the temporal structure of noise presentation, i.e., short bursts or continuously. Interestingly, noise bursts enhanced excitation and inhibition, but irrespective of frequency, leaving excitatory-inhibitory correlation unaltered.

Patterned stimulation dramatically changed spike output, in terms of spike timing precision and tuning curve structure. We made 22 whole-cell current-clamp or cell-attached recordings from P12-P21 or adult AI neurons *in vivo*. Spike firing was imprecise during P12-P21 (Supplementary Fig. 7a), such that latency was highly variable from trial to trial. Spike timing was much more precise in adults (Supplementary Fig. 7b), tightly locked to tone onset. Patterned stimulation increased spike output and enhanced temporal precision in young animals but not adults (Supplementary Figs. 7c-e), as predicted from simulations<sup>12</sup> (Supplementary Fig. 7f). Surprisingly, while maturation and plasticity of excitatory and inhibitory responses predicted much of action potential generation and spiking receptive field development, synaptic inputs by themselves did not seem to fully predict the absolute values of spike latency and variability. Thus development of other factors (e.g., ion channel expression<sup>22</sup>) play important roles in coupling cortical synaptic input to spiking output.

Lastly, we asked whether accelerated balancing of excitatory and inhibitory inputs through patterned stimulation was sufficient to prevent further modifications of synaptic receptive fields. We performed three final experiments to probe the limits and duration of cortical plasticity in relation to excitatory-inhibitory balance.

We first measured synaptic tuning before and after an initial episode of patterned stimulation, followed by another round of patterned stimulation ~30 minutes later to determine if additional modifications were induced. An example P18 cell is shown in Figure 5. Initially, excitation and inhibition were weakly correlated due to low selectivity of inhibition (Fig. 5a;  $r_{pre}$ : 0.27). Patterned stimulation with 4 kHz tones increased excitation, inhibition, and excitatory-inhibitory correlation (Fig. 5b;  $r_{post1}$ : 0.77). Thirty minutes later, a second episode of 4 kHz patterned stimulation was presented, but tuning was not significantly changed (Fig. 5c;  $r_{post2}$ : 0.82).

Therefore, relatively brief episodes of structured sensory experience during development reorganize AI synaptic receptive fields, first limiting and eventually preventing subsequent patterned stimulation from triggering further modifications. After first modifying excitation and inhibition, no additional changes were induced by a second period of patterned stimulation (Fig. 5d), as by then the coupling between excitation and inhibition had reached mature levels.

To more completely determine the temporal dynamics of these effects, we made consecutive recordings from the same animals for hours after one round of patterned stimulation (Supplementary Fig. 8). For example, recordings in Supplementary Figure 8a-c were made in the same P17 animal. Initially, excitatory-inhibitory correlation was low (Supplementary Fig. 8a;  $r_{pre}$ : 0.22). Twenty-five minutes after 1 kHz patterned stimulation, correlation in a second neuron was much higher (Supplementary Fig. 8b;  $r_{post1}$ : 0.98); but two hours later,

correlation in a third neuron was reduced (Supplementary Fig. 8c;  $r_{post2}$ : 0.54). Seemingly regardless of location within AI, patterned stimulation increased excitatory-inhibitory correlation for hours before returning to initial lower levels (Supplementary Fig. 8d).

Previous studies indicate that prolonged exposure to random stimuli can undo or extinguish prior modifications to neural circuits, potentially leaving maps and receptive fields in unrefined yet plastic states<sup>4,19</sup>. Conversely, a few days of exposure to tonal stimuli early in life can profoundly affect AI topography and receptive fields, lasting days to months afterward<sup>3,7</sup>. In our final experiment, we therefore used much longer periods of patterned stimulation, to examine conditions for AI critical period closure.

Rat pups (P9-P11) were repetitively exposed to 2 kHz or 7 kHz tones for one to three days in their home cages<sup>7</sup>. We then made recordings in anesthetized P12-P16 animals, comparing synaptic receptive fields (as in Fig. 1) and degree of exposure-induced synaptic modifications (as in Fig. 3) to age-matched controls.

Early exposure to pure tones accelerated development of excitatory-inhibitory balance and prevented subsequent patterned stimulation from inducing synaptic modifications (Supplementary Fig. 9). The cell shown in Supplementary Figure 9a was recorded from a P16 animal exposed to repetitive 2 kHz tones from P11-P14. Correlation between excitation and inhibition ( $r_{pre}$ : 0.66) was high, presumably due to the prior structured sensory exposure. After measuring synaptic tuning, we repetitively presented 16 kHz tones for five minutes, but patterned stimulation did not significantly change synaptic strength or excitatory-inhibitory balance ( $r_{post}$ : 0.64).

Early exposure to repetitive tonal stimuli for a few days enhanced average excitatory-inhibitory correlation at P12-P16 compared to similarly aged animals raised under normal laboratory acoustic conditions (Supplementary Fig. 9b). This precocious maturation of synaptic receptive fields occurred in absence to changes to cell-intrinsic properties such as input resistance and synaptic kinetics (Supplementary Fig. 9c). Furthermore, this accelerated development prevented changes in synaptic strength and balance by additional periods of patterned stimulation during recording (Supplementary Fig. 9d). These data indicate that accumulation of sensory experience early in development, when excitation and inhibition are still uncorrelated, rapidly improves the balance and structure of synaptic receptive fields, preventing additional exposure-induced changes from occurring; in essence, ending the critical period of heightened cortical plasticity.

In conclusion, we have defined here the AI critical period as that developmental stage when brief episodes of structured sensory experience dramatically alter synaptic receptive fields. During this period, patterned tonal stimulation sets in motion a coordinated set of bidirectional modifications to specific elements of synaptic receptive fields which endure for hours (after minutes of exposure) or weeks (after days of exposure). Synaptic modifications could be forms of spike-timing-dependent plasticity<sup>23-25</sup>, heterosynaptic plasticity<sup>26-28</sup> or homeostatic changes such as synaptic scaling<sup>29</sup>. Together, these maturational adjustments dynamically fine-tune cortical networks, balancing excitatory and inhibitory inputs to reduce

the efficacy of sensory stimuli in modifying synaptic strength and receptive fields later in life.

Our results demonstrate that maturation of inhibitory circuitry is not simply expressed as an overall increase in inhibitory strength with age. Rather, inhibition is strong early in life, but is initially poorly tuned for spectral features, unmatched to excitatory inputs. Another recent study<sup>30</sup> also found that inhibition was high shortly after hearing onset, but that many neurons in layer 4 of AI seemed to have pre-balanced excitatory and inhibitory synaptic receptive fields. Here we found that, while in some neurons, excitation and inhibition were similarly balanced at young ages (Fig. 1c), in different cells even from the same animals, excitatory-inhibitory co-tuning and correlation could be much lower. Various components of cortical receptive fields may develop at different rates, such as frequency tuning curves at other intensity levels. Likewise, different cortical layers, sectors, or microcircuits within AI might also have differential developmental trajectories or sensitivity to the acoustic environment. Thus, overall, the progressive balancing of excitation and inhibition is apparently a network-level phenomenon. Consistent experience with reliable, patterned sensory stimulation refines intracortical inhibition precisely in proportion to excitation. The progressive remodeling of inhibitory receptive fields by sensory experience leads to balanced synaptic activity in cortical networks and limits further exposure-induced modifications, closing the developmental critical period. Given the importance of balanced excitation and inhibition for the temporal precision of activity in the auditory cortex<sup>12,13</sup>, failure of this maturational adjustment to occur could be catastrophic for development of speech and language skills, with lasting consequences such as dyslexia or other development-associated language impairments<sup>5, 10</sup>.

## Methods

Sprague-Dawley rats were anesthetized with ketamine/xylazine. AI was located by mapping multiunit spike responses. *In vivo* whole-cell recordings were performed and analyzed as previously described<sup>12-15</sup>. In Figure 4d, “presented only” contributions were determined from changes to presented tones themselves, assuming that other responses remained unchanged. “Unpresented only” contributions were determined by assuming that after patterned stimulation, only responses to unpresented tones were affected. Spike timing precision (Supplementary Figure 7) was quantified as standard deviation of latency to first tone-evoked spike (‘jitter’).

## Methods

### Surgical preparation

All experimental procedures used in this study were approved under UCSF IACUC protocols. Experiments were carried out in a sound-attenuating chamber. Sprague-Dawley rats were anesthetized with ketamine/xylazine. As ketamine is a low-affinity NMDA receptor antagonist, the extent of experience-dependent synaptic modifications reported here may be underestimated. The location of AI in the right hemisphere was determined by mapping multiunit spike responses at 400-800  $\mu\text{m}$  below the surface using parylene-coated tungsten electrodes: AI neurons spike at short latency (8-16 ms) to the best frequency and

are tonotopically organized from high to low frequency along the anterior-posterior axis<sup>7,14,15</sup>.

### Whole-cell recording

*In vivo* whole-cell recordings were obtained from neurons located approximately 400-1100  $\mu\text{m}$  below the pial surface<sup>12-15</sup>. For cells recorded between P12-P21, there was no significant correlation between recording depth and excitatory-inhibitory correlation ( $r^2$ : 0.08,  $p > 0.2$ ). Cortical pulsations were prevented with 4% agar. Recordings were made with an AxoClamp 2B or MultiClamp 700B (Molecular Devices). Patch pipettes (4-9M $\Omega$ ) contained (in mM): 125 Cs-gluconate, 5 TEACl, 4 MgATP, 0.3 GTP, 10 phosphocreatine, 10 HEPES, 0.5 EGTA, 3.5 QX-314, 2 CsCl, pH 7.2 (voltage-clamp) or: 135 K-gluconate, 5 NaCl, 5 MgATP, 0.3 GTP, 10 phosphocreatine, 10 HEPES, 0.5 EGTA, pH 7.3 (current-clamp). For the experiments shown in Fig. 1,  $R_s$  was  $27.4 \pm 10.0$  M $\Omega$  (s.d.) between P12-P21 and  $23.6 \pm 9.8$  M $\Omega$  in adults, and  $R_i$  was  $155.3 \pm 71.8$  M $\Omega$  between P12-P21 and  $110.7 \pm 54.0$  M $\Omega$  in adults, determined by monitoring cells with brief hyperpolarizing voltage steps ( $-10$  mV, 100 ms). Cells were excluded if  $R_i$  or  $R_s$  changed  $>30\%$  over the entire experiment (Supplementary Fig. 4). Data were filtered at 2 kHz, digitized at 10 kHz, and analyzed with Clampfit 10 (Molecular Devices) and Matlab (The MathWorks). Sensory stimulation consisted of a pseudo-random sequence of pure tones (0.5-32 kHz at one octave intervals, 50 ms duration, 70 dB intensity, 0.5 Hz rate). We measured synaptic currents at two to five different holding potentials ( $-90$ ,  $-70$ ,  $-40$ ,  $-20$ , and 0 mV), and computed the excitatory and inhibitory synaptic conductances as previously described<sup>12-15</sup>. Excitation was measured as the mean of a 1-2 msec window centered on the peak ( $\sim 10$ -20 msec after tone onset) and inhibition was measured as the mean of a 10 msec window  $\sim 25$ -40 msec after tone onset. Statistical comparisons were made using Student's t-test. We focused on the period between P12-P21 for statistical analysis so that sample sizes between young and adult animals would be similar and because prior *in vitro* studies have indicated that synaptic connections develop anatomically and physiologically during this time<sup>16,17</sup>.

In Figures 2 and 4 and Supplementary Figure 3, we normalized excitatory and inhibitory responses to the conductance values of the maximal amount of excitation and inhibition, respectively. In Figure 4 and Supplementary Figure 3, conductances were plotted in octaves ( $\log_2$  of tone frequency) relative to the excitatory and inhibitory best frequencies. In Figure 4d, we first determined the contribution to the increase in excitatory-inhibitory correlation from the changes to the presented tone by itself (Fig. 4d, "presented only"). In this case, we assumed that after patterned stimulation, the responses to all other tones remained at their original values before patterned stimulation, and calculated the corresponding excitatory-inhibitory correlation. Then to determine the contribution of changes to all other inputs (Fig. 4d, "unpresented only"), we assumed that after patterned stimulation, only the responses to the unpresented tones were affected, while the responses to the presented tone itself stayed at their initial levels, and again calculated the change in excitatory-inhibitory correlation. In the studies shown in Supplementary Figures 6 and 9, experimenters were not blind to the exposure status of each animal. For the experiments in Supplementary Figure 7, spike timing precision was quantified as the standard deviation of the latency to the first tone-evoked spike ('jitter').



The simulations summarized in Supplementary Figure 7f used a conductance-based integrate-and-fire neuron with parameters fit from our experiments. Spike generation in cortical neurons is a complex function that depends on many other factors not directly studied here, such as anesthetic state and ion channel expression patterns. Regardless, simulating the synaptic dynamics alone in essence recapitulated the major features of developmental changes to AI spiking described here- decrease in spike timing variability and increase in spiking probability. Membrane voltage was computed as:

$$\tau_m \frac{dV}{dt} = V_{rest} - V + g_e(t)(E_e - V) + g_i(t)(E_i - V),$$

with membrane time constant  $\tau_m=10$  msec, resting membrane potential  $V_{rest}=-60$  mV, excitatory reversal potential  $E_e=0$  mV, and inhibitory reversal potential  $E_i=-70$  mV. A spike was evoked in the postsynaptic neuron if the membrane voltage reached threshold of  $-45$  mV, at which point the membrane potential was returned to  $V_{rest}$  in the next time step.

The postsynaptic neuron received 10 excitatory inputs and 10 inhibitory inputs, each with synaptic conductances  $g_e$  and  $g_i$ , decay time constants  $\tau_{e\_decay}$  and  $\tau_{i\_decay}$ , and presynaptic latencies  $e_t$  and  $i_t$ . Different sets of parameters were used to simulate the four experimental conditions of spike firing before and after patterned stimulation in young and adult neurons. For simulating tone-evoked spiking in young neurons before repetitive tonal exposure,  $g_e=0.1441$  nS for each of the 10 excitatory inputs (conductance values from Supplementary Figure 3d, bottom),  $g_i=0.2072$  nS for each of the 10 inhibitory inputs (from Supplementary Figure 3d, bottom), and decay time constants were  $\tau_{e\_decay}=23.3$  msec and  $\tau_{i\_decay}=95.8$  msec (averaged over all P12-P21 recordings from Supplementary Figures 4a and 4b). Presynaptic spike arrival times were drawn from a normal distribution with means and standard deviations  $e_t=12.7\pm 5.6$  msec and  $i_t=17.7\pm 5.8$  msec (from Supplementary Figures 4d and 4e). For spiking in adult neurons before patterned stimulation,  $g_e=0.1112$  nS and  $g_i=0.1414$  nS for each input (from Supplementary Figure 3d, bottom), with decay time constants  $\tau_{e\_decay}=16.6$  msec and  $\tau_{i\_decay}=60.6$  msec (from Supplementary Figures 4a and 4b). Presynaptic spike arrival times were  $e_t=10.0\pm 2.9$  msec and  $i_t=12.6\pm 3.7$  msec (from Supplementary Figures 4d and 4e). To simulate the synaptic effects induced by patterned stimulation, for young neurons,  $g_e=0.2351$  nS,  $g_i=0.3168$  nS,  $e_t=8.6\pm 2.8$  msec, and  $i_t=13.3\pm 3.8$  msec; for adult neurons,  $g_e=0.117$  nS,  $g_i=0.1416$  nS, while  $e_t$  and  $i_t$  were unaltered. These adjusted values of conductance and latency are taken from the results of Figure 3 and Supplementary Figure 4f. Spike counts and timing jitter were determined from 50 trials (approximately the number of trials used for measuring these values in the experiments).

## Supplementary Material

Refer to Web version on PubMed Central for supplementary material.

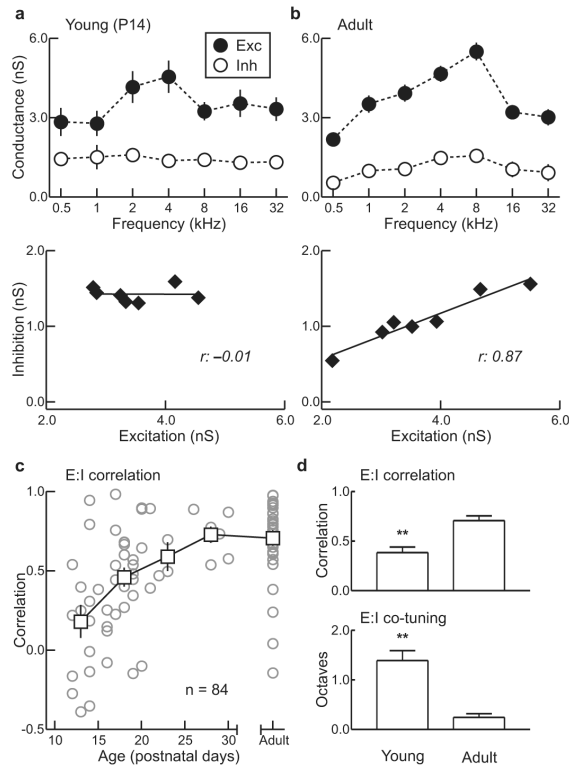
## Acknowledgements

We thank C. A. Atencio, T. Babcock, E. Chang, E. de Villers-Sidani, M. R. DeWeese, G. Ehret, S. Gandhi, K. Imaizumi, M. M. Merzenich, C. Niell, A.-M. Oswald, and A. Y. Tan for comments, discussions, and technical assistance. This work was supported by the NIDCD, the Conte Center for Neuroscience Research at UCSF, Hearing Research Inc., and the John C. and Edward Coleman Fund. R.C.F. is a recipient of a NIDCD K99/R00 Career Award, a Jane Coffin Childs Postdoctoral Research Fellowship, and a Sandler Translational Research Fellowship.

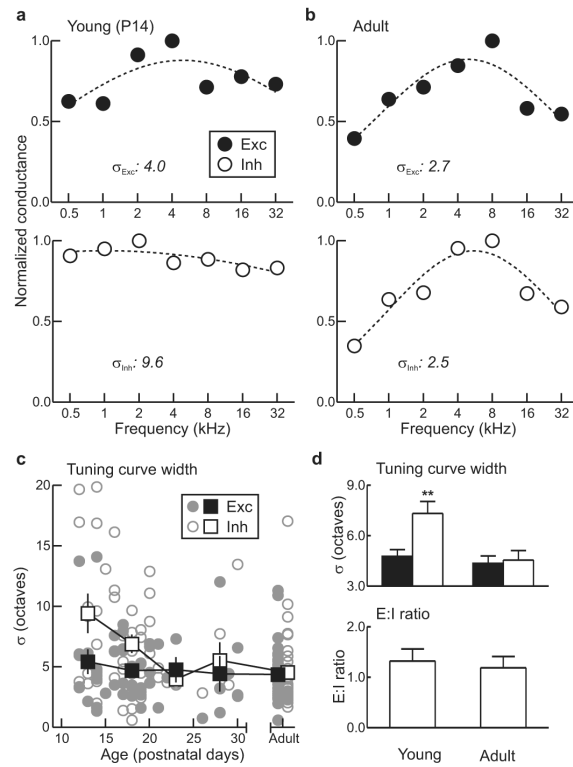
## References

1. Katz LC, Shatz CJ. Synaptic activity and the construction of cortical circuits. *Science*. 1996; 274:1133–1138. [PubMed: 8895456]
2. Miller KD. Synaptic economics: competition and cooperation in synaptic plasticity. *Neuron*. 1996; 17:371–374. [PubMed: 8816700]
3. Zhang LI, Bao S, Merzenich MM. Persistent and specific influences of early acoustic environments on primary auditory cortex. *Nat Neurosci*. 2001; 4:1123–1130. [PubMed: 11687817]
4. Chang EF, Merzenich MM. Environmental noise retards auditory cortical development. *Science*. 2003; 300:498–502. [PubMed: 12702879]
5. Rubenstein JL, Merzenich MM. Model of autism: increased ratio of excitation/inhibition in key neural systems. *Genes Brain Behav*. 2003; 2:255–267. [PubMed: 14606691]
6. Hensch TK. Critical period plasticity in local cortical circuits. *Nat Rev Neurosci*. 2005; 6:877–888. [PubMed: 16261181]
7. de Villers-Sidani E, Chang EF, Bao S, Merzenich MM. Critical period for spectral tuning defined in the primary auditory cortex (A1) of the rat. *J Neurosci*. 2007; 27:180–189. [PubMed: 17202485]
8. Huberman AD, Feller MB, Chapman B. Mechanisms underlying development of visual maps and receptive fields. *Annu Rev Neurosci*. 2008; 31:479–509. [PubMed: 18558864]
9. Doupe AJ, Kuhl PK. Birdsong and human speech: common themes and mechanisms. *Annu Rev Neurosci*. 1999; 22:567–631. [PubMed: 10202549]
10. Tallal P, Benasich AA. Developmental language learning impairments. *Dev Psychopathol*. 2002; 14:559–579. [PubMed: 12349874]
11. Shu Y, Hasenstaub A, McCormick DA. Turning on and off recurrent balanced cortical activity. *Nature*. 2003; 423:288–293. [PubMed: 12748642]
12. Wehr M, Zador AM. Balanced inhibition underlies tuning and sharpens spike timing in auditory cortex. *Nature*. 2003; 426:442–446. [PubMed: 14647382]
13. Tan AY, Zhang LI, Merzenich MM, Schreiner CE. Tone-evoked excitatory and inhibitory synaptic conductances of primary auditory cortex neurons. *J Neurophysiol*. 2004; 92:630–643. [PubMed: 14999047]
14. Froemke RC, Merzenich MM, Schreiner CE. A synaptic memory trace for cortical receptive field plasticity. *Nature*. 2007; 450:425–429. [PubMed: 18004384]
15. Kenet T, Froemke RC, Schreiner CE, Pessah IN, Merzenich MM. Perinatal exposure to a noncoplanar polychlorinated biphenyl alters tonotopy, receptive fields, and plasticity in rat primary auditory cortex. *Proc Natl Acad Sci USA*. 2007; 104:7646–7651. [PubMed: 17460041]
16. Luhmann HJ, Prince DA. Postnatal maturation of the GABAergic system in rat neocortex. *J Neurophysiol*. 1991; 65:247–263. [PubMed: 1673153]
17. Oswald AM, Reyes A. Maturation of intrinsic and synaptic properties of layer 2/3 pyramidal neurons in mouse auditory cortex. *J Neurophysiol*. 2008; 99:2998–3008. [PubMed: 18417631]
18. Gandhi SP, Yanagawa Y, Stryker MP. Delayed plasticity of inhibitory neurons in developing visual cortex. *Proc Natl Acad Sci USA*. 2008; 105:16797–16802. [PubMed: 18940923]
19. Chang EF, Bao S, Imaizumi K, Schreiner CE, Merzenich MM. Development of spectral and temporal response selectivity in the auditory cortex. *Proc Natl Acad Sci USA*. 2005; 102:16460–16465. [PubMed: 16263924]
20. Smith SL, Trachtenberg JT. Experience-dependent binocular competition in the visual cortex begins at eye opening. *Nat Neurosci*. 2007; 10:370–375. [PubMed: 17293862]
21. Stern EA, Maravall M, Svoboda K. Rapid development and plasticity of layer 2/3 maps in rat barrel cortex in vivo. *Neuron*. 2001; 31:305–315. [PubMed: 11502260]
22. Spitzer NC. Ion channels in development. *Annu Rev Neurosci*. 1979; 2:363–395. [PubMed: 395884]
23. Froemke RC, Tsay IA, Raad M, Long JD, Dan Y. Contribution of individual spikes in burst-induced long-term synaptic modification. *J Neurophysiol*. 2006; 95:1620–1629. [PubMed: 16319206]

24. Meliza CD, Dan Y. Receptive-field modification in rat visual cortex induced by paired visual stimulation and single-cell spiking. *Neuron*. 2006; 49:183–189. [PubMed: 16423693]
25. Jacob V, Brasier DJ, Erchova I, Feldman D, Shulz DE. Spike timing-dependent synaptic depression in the in vivo barrel cortex of the rat. *J Neurosci*. 2007; 27:1271–1284. [PubMed: 17287502]
26. Nishiyama M, Hong K, Mikoshiba K, Poo MM, Kato K. Calcium stores regulate the polarity and input specificity of synaptic modification. *Nature*. 2000; 408:584–588. [PubMed: 11117745]
27. Royer S, Paré D. Conservation of total synaptic weight through balanced synaptic depression and potentiation. *Nature*. 2003; 422:518–522. [PubMed: 12673250]
28. Lin Y, et al. Activity-dependent regulation of inhibitory synapse development by Npas4. *Nature*. 2008; 455:1198–1204. [PubMed: 18815592]
29. Turrigiano GG, Nelson SB. Homeostatic plasticity in the developing nervous system. *Nat Rev Neurosci*. 2004; 5:97–107. [PubMed: 14735113]
30. Sun YJ, et al. Fine-tuning of pre-balanced excitation and inhibition during auditory cortical development. *Nature*. in press.

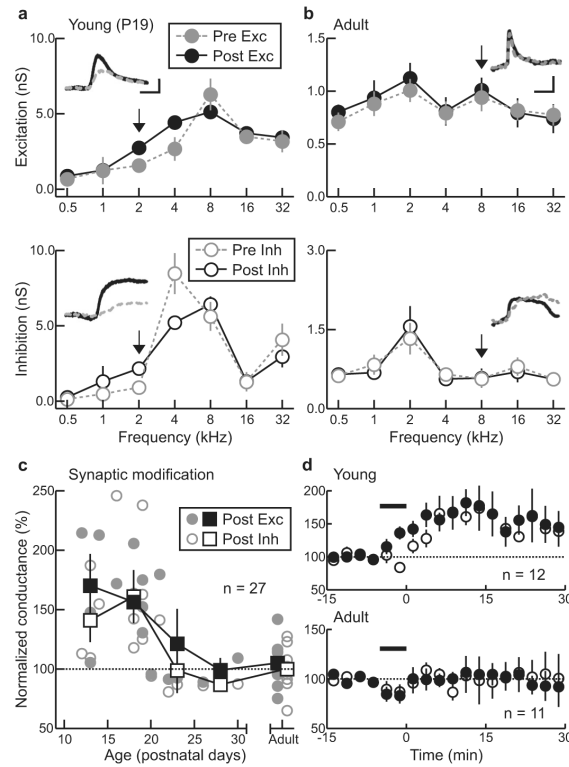


**Figure 1.** Refinement of excitatory-inhibitory balance during AI critical period. **a**, Imbalanced synaptic frequency tuning at P14. Top, frequency tuning of excitation (filled) and inhibition (open). Bottom, excitation and inhibition were uncorrelated (linear correlation coefficient  $r = -0.01$ ,  $p > 0.8$ ). **b**, Balanced tone-evoked excitation and inhibition in adults. Top, frequency tuning. Bottom, excitation and inhibition were correlated ( $r = 0.87$ ,  $p < 0.001$ ). **c**, Increase of excitatory-inhibitory balance during AI critical period. Circles, individual recordings. Squares, averages. **d**, Summary of developmental changes to excitatory-inhibitory balance. Top, excitatory-inhibitory correlation in young and adults (P12-P21,  $r = 0.37 \pm 0.06$ ,  $n = 43$ ; adults,  $r = 0.71 \pm 0.05$ ,  $n = 31$ ,  $p < 10^{-4}$  compared to P12-P21, Student's two-tailed t-test). \*\*,  $p < 0.01$ . Bottom, difference in excitatory and inhibitory best frequencies in young and adults (P12-P21, best frequency difference:  $1.4 \pm 0.2$  octaves,  $n = 43$ ; adults,  $0.2 \pm 0.1$  octaves,  $n = 25$ ,  $p < 10^{-6}$ ). Error bars, s.e.m.



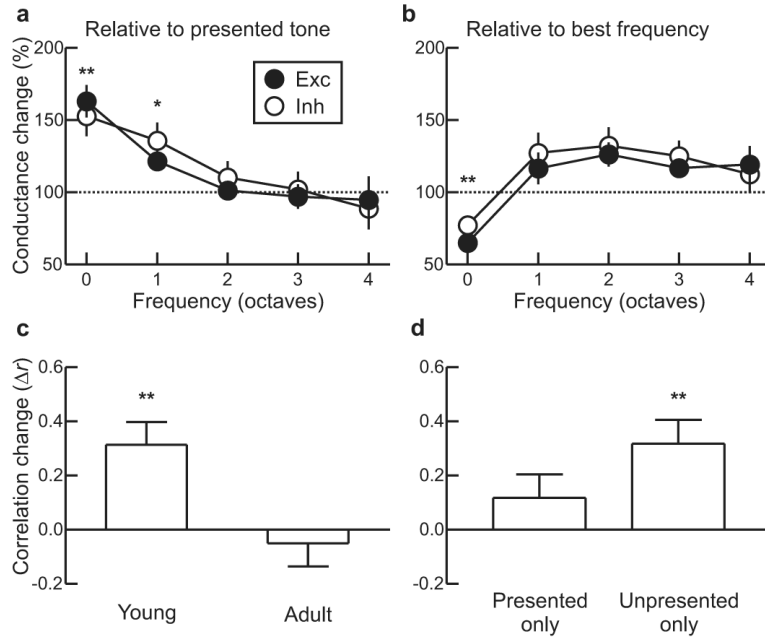
**Figure 2.**

Delayed maturation of inhibitory frequency tuning. **a**, Excitatory frequency tuning was sharper than inhibitory tuning at P14. Lines, Gaussian fits ( $\sigma_{Exc}$ : 4.0,  $\sigma_{Inh}$ : 9.6). Same recording as in Figure 1a. **b**, Excitatory and inhibitory tuning were both sharp in adulthood ( $\sigma_{Exc}$ : 2.7,  $\sigma_{Inh}$ : 2.5). Same recording as in Figure 1b. **c**, Excitatory frequency tuning sharpened before inhibition (P12-P15,  $\sigma_{Exc}$ :  $5.4 \pm 1.0$ ,  $\sigma_{Inh}$ :  $9.4 \pm 1.6$ ,  $n=15$ ,  $p < 0.02$ ). Circles, excitation (filled) and inhibition (open) for each cell. Squares, averages. **d**, Summary of developmental changes to tuning. Top, tuning sharpness in young (P12-P21,  $\sigma_{Exc}$ :  $4.9 \pm 0.4$ ,  $\sigma_{Inh}$ :  $7.7 \pm 0.8$ ,  $n=43$ ,  $p < 0.0004$ ) and adults ( $\sigma_{Exc}$ :  $4.4 \pm 0.4$ ,  $\sigma_{Inh}$ :  $4.5 \pm 0.6$ ,  $n=31$ ,  $p > 0.8$ ). Bottom, excitation-to-inhibition ratio (E:I ratio) was unchanged during AI critical period. E:I ratios were similar between young (P12-P21, E:I ratio:  $1.3 \pm 0.2$ ,  $n=43$ ) and adults (E:I ratio:  $1.2 \pm 0.2$ ,  $n=31$ ,  $p > 0.6$ ). Error bars, s.e.m.

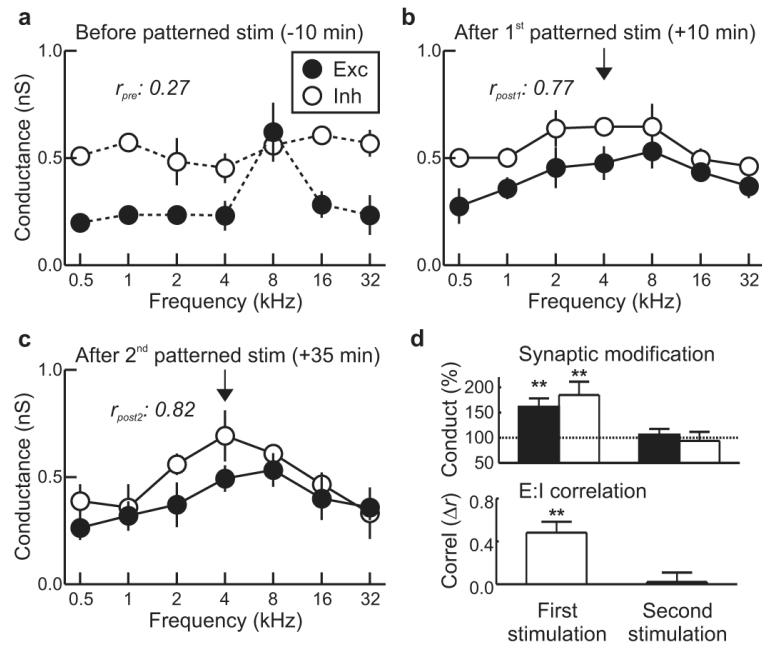


**Figure 3.**

Patterned stimulation rapidly enhanced excitation and inhibition during P12- P21. **a**, Long-term synaptic enhancement at P19. Before patterned 2 kHz stimulation, excitation and inhibition were moderately correlated ( $r_{pre}$ : 0.57); after stimulation, correlation increased ( $r_{post}$ : 0.86). Top, excitation at 2 kHz increased after patterned stimulation (enhancement of 75.2%,  $p < 0.05$ ). Insets, conductances evoked by 2 kHz before (gray) and after (black) repetitive stimulation. Arrow, frequency chosen for patterned stimulation. Scale bars, 1 nS, 40 msec. Bottom, inhibition at 2 kHz increased after repetitive stimulation (enhancement of 138.5%,  $p < 0.05$ ). **b**, Patterned stimulation did not affect adult AI. Top, excitation was unaltered after 8 kHz patterned stimulation (enhancement of 7.4%,  $p > 0.3$ ). Scale bars, 0.5 nS, 40 msec. Bottom, inhibition at 8 kHz remained unchanged (enhancement of 1.8%,  $p > 0.3$ ). Excitatory-inhibitory correlation was unaffected ( $r_{pre}$ : 0.68,  $r_{post}$ : 0.74). **c**, Critical period for synaptic modifications induced by patterned stimulation. Circles, changes to excitation (filled) or inhibition (open) for each recording. **d**, Time course of synaptic modifications to tone presented during patterned stimulation. Top, P12-P21 (excitation:  $63.1 \pm 11.3\%$ ,  $n = 12$ ,  $p < 0.0002$ ; inhibition:  $52.9 \pm 14.1\%$ ,  $p < 0.004$ ). Horizontal bar, patterned stimulation. Bottom, adults (excitation:  $5.2 \pm 5.3\%$ ,  $n = 11$ ,  $p > 0.3$ ; inhibition:  $0.2 \pm 5.1\%$ ,  $p > 0.9$ ). Error bars, s.e.m.

**Figure 4.**

Patterned stimulation improved excitatory-inhibitory coupling by coordinated synaptic modifications across multiple inputs. **a**, Synaptic modifications at the presented tone frequency spread to other inputs within one octave (excitation one octave from presented frequency:  $21.6 \pm 6.7\%$ ,  $n=12$ ,  $p<0.01$ ; inhibition:  $36.0 \pm 12.5\%$ ,  $p<0.02$ ), but not 2+ octaves away ( $p>0.3$ ). \*\*,  $p<0.01$ ; \*,  $p<0.05$ . **b**, After patterned stimulation, responses at original best frequency were reduced (excitation:  $-34.8 \pm 6.4\%$ ,  $n=12$ ,  $p<0.0003$ ; inhibition:  $-22.7 \pm 6.1\%$ ,  $p<0.004$ ). **c**, Patterned stimulation increased excitatory-inhibitory correlation in young ( $r: 0.31 \pm 0.08$ ,  $n=12$ ,  $p<0.004$ ) but not adults ( $r: -0.03 \pm 0.09$ ,  $n=11$ ,  $p>0.7$ ). **d**, Nonspecific modifications across multiple inputs were predominant for balancing excitation and inhibition. Considered separately, synaptic modifications only at the presented frequency were less effective (“presented only”,  $r: 0.12 \pm 0.09$ ,  $p>0.2$ ) than changes to all other inputs (“unpresented only”,  $r: 0.32 \pm 0.09$ ,  $p<0.004$ ). Error bars, s.e.m.

**Figure 5.**

/B> Patterned stimulation prevented additional synaptic modifications. **a**, Synaptic tuning before first episode of patterned stimulation. Initially, excitatory-inhibitory correlation was low ( $r_{pre} = 0.27$ ). **b**, Same cell as in **a**, but after first period of 4 kHz patterned stimulation. Excitation and inhibition at 4 kHz were enhanced and excitatory-inhibitory correlation increased (excitation: 108.7%,  $p < 0.03$ ; inhibition: 44.4%,  $p < 0.05$ ;  $r_{post1} = 0.77$ ). **c**, Same cell as in **a**, but after second period of 4 kHz repetitive stimulation. Excitatory-inhibitory strength and balance were unaffected (excitation: 2.1%,  $p > 0.4$ ; inhibition: 6.2%,  $p > 0.3$ ;  $r_{post2} = 0.82$ ). **d**, Summary. Top, conductance changes at presented tone frequency after first (excitation:  $61.4 \pm 16.7\%$ ,  $n = 5$ ,  $p < 0.03$ ; inhibition:  $84.8 \pm 26.5\%$ ,  $p < 0.04$ ) and second (excitation:  $6.2 \pm 11.4\%$ ,  $n = 5$ ,  $p > 0.6$ ; inhibition:  $-6.2 \pm 18.0\%$ ,  $p > 0.7$ ) stimulation periods. Bottom, change in excitatory-inhibitory correlation after first ( $r = 0.48 \pm 0.10$ ,  $p < 0.01$ ) and second ( $r = 0.02 \pm 0.09$ ,  $p > 0.8$ ) stimulation periods. Error bars, s.e.m.